Molecular Therapy
Nucleic Acids
Original Article

Smooth muscle cell-targeted RNA ligand promotes accelerated reendothelialization in a swine peripheral injury model

Beilei Lei,[1,2] Linda B. Liu,[3] Lauren Stokes,[3] Paloma H. Giangrande,[4] Francis J. Miller, Jr.,[5,6] and Saami K. Yazdani[3]

[1]Department of Medicine, Wake Forest University School of Medicine, Winston-Salem, NC, USA; [2]Department of Medicine, Duke University, Durham, NC, USA; [3]Department of Engineering, Wake Forest University, Winston-Salem, NC, USA; [4]Wave Life Sciences, Cambridge, MA, USA; [5]Veterans Administration Medical Center, Nashville, TN, USA; [6]Department of Medicine, Vanderbilt University Medical Center, Nashville, TN, USA

The local delivery of antiproliferative agents to inhibit neointimal growth is not specific to vascular smooth muscle cells (VSMC) and delays reendothelialization and vascular healing. This investigation was intended to evaluate the effect of luminal delivery of a VSMC-specific aptamer on endothelial healing. The impact of an RNA aptamer (Apt 14) was first examined on the migration and proliferation of primary cultured porcine aortic endothelial cells (ECs) in response to *in vitro* scratch wound injury. We further evaluated the impact of Apt 14 on reendothelialization when delivered locally in a swine iliofemoral injury model. Although Apt 14 did not affect EC migration and proliferation, *in vitro* results confirmed that paclitaxel significantly inhibited EC migration and proliferation. En face scanning electron microscopy demonstrated confluent endothelium with elongated EC morphology in Apt 14-treated arteries 14 and 28 days post-treatment. In contrast, vessels treated with paclitaxel-coated balloons displayed a cobblestone morphology and significant platelet and fibrin attachment at cell junctions. These results provide the first evidence of the efficacy of a cell-targeted RNA aptamer to facilitate endothelial healing in a clinically relevant large animal model.

INTRODUCTION

Peripheral arterial disease (PAD), which costs the United States greater than $20 billion annually, affects more than eight million people.[1] The major challenge with PAD is that current treatment options often fail, thus necessitating for repeat surgeries or interventional procedures.[2–5] Percutaneous interventions, including stenting and balloon angioplasty, are the preferred choice to treat patients with PAD, as they offer reduced mortality, morbidity, and length of hospital stay compared to surgery.[6,7] However, a larger number of interventional treatments fail within 2 years, with 50%–85% of patients developing significant restenosis and 16%–65% of targeted vessels occulding.[5,8] The use of antiproliferative drugs in combination with bare-metal stents (BMSs), that is, drug-eluting stents (DESs), has been a major breakthrough in the treatment of patients with coronary artery disease.[9,10] However, stents perform poorly in treating patients with PAD. Metallic stents are subjected to both mechanical stress and severe deformation given that the arteries in the periphery twist, bend, and shorten. This leads to frequent stent fractures (up to 68%) and restenosis rates.[11] In addition, drugs eluted from stents are constrained by the platform design and deliver drugs to only <20% of the arterial surface.[12]

Newer technologies have emerged to overcome the limitations of stents. Drug-coated balloons (DCBs) provide an alternative therapeutic approach to treat patients with PAD and allow interventionalists the ability to "leave nothing behind," preserving future treatment options. However, clinical results have been inconsistent, with recent studies showing safety concerns and an increased risk for death and amputations in patients treated with paclitaxel-coated balloons.[13]

Although PAD delivery platforms have changed significantly over the past decade, PAD therapeutic drugs have not. All DESs and DCBs are designed to deliver the antiproliferative agent paclitaxel or a limus (e.g., sirolimus, everolimus, zotarolimus) to the luminal surface to inhibit restenosis. However, studies have shown that the nonspecific effects of these antimitotic drugs adversely affect endothelial cells (ECs), impairing reendothelialization and leading to late stent thrombosis and death.[14,15] Therefore the goal of this study was to investigate a cell-specific therapeutic alternative that can overcome the nonspecific effects of the current antimitotic drugs. We previously identified a vascular smooth muscle cell (VSMC)-targeted RNA aptamer (Apt 14) that attenuated neointimal formation in a mouse carotid injury model.[16] Furthermore, we showed that Apt 14 delivered intraluminally inhibited neointimal growth in a clinically relevant swine iliofemoral injury model.[17] In this study, we extended these findings to test the ability of Apt 14 to facilitate vascular healing in a clinically relevant swine model of PAD.

Received 21 June 2023; accepted 23 August 2023;
https://doi.org/10.1016/j.omtn.2023.08.025.

Correspondence: Saami K. Yazdani, Department of Engineering, Wake Forest University, 455 Vine Street, Winston-Salem, NC 27101, USA.
E-mail: yazdanis@wfu.edu

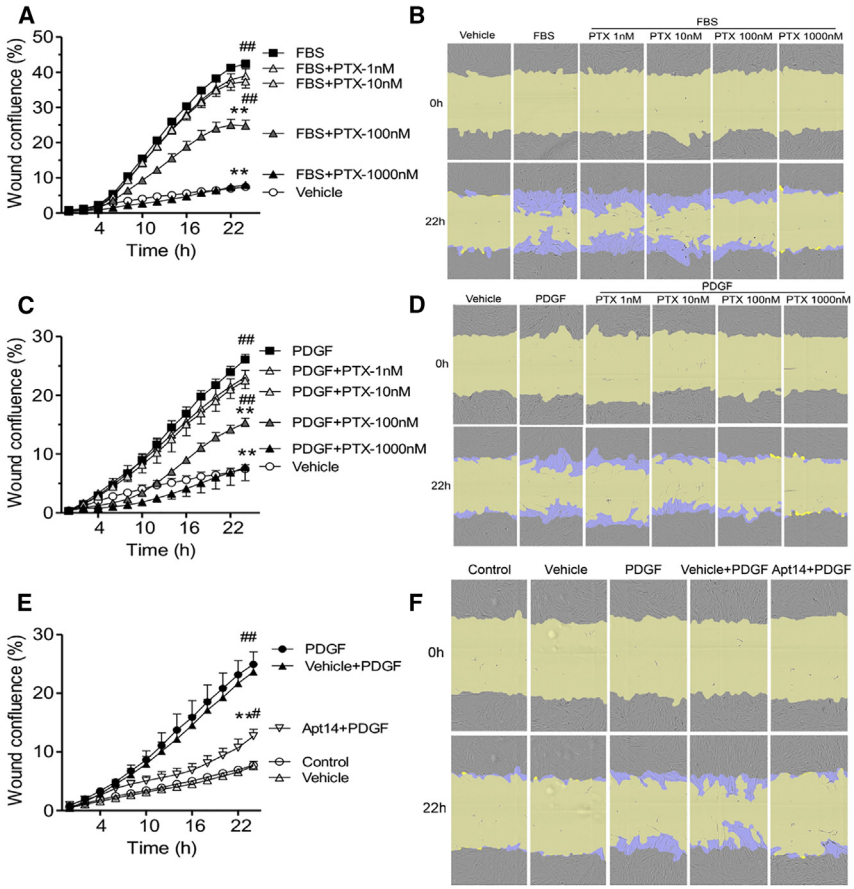

Figure 1. Effects of paclitaxel (PTX) and RNA aptamer Apt 14 on porcine aortic smooth muscle cell (SMC) migration

Cells were cultured to confluence followed by two days of serum starvation, subjected to scratch wound injury, and treated with fetal bovine serum (FBS; 5%) (A) or platelet-derived growth factor-BB (PDGF; 5 ng/mL) (C) following PTX (1–1,000 nM) or with Apt 14 (200 nM) following PDGF (5 ng/mL) (E). Migration was assessed on the basis of wound confluence using the IncuCyte S3 system. (B, D, and F) Representative cell-phase images show wound confluence at 0 and 22 h after FBS or PDGF exposure. The initial scratch wound and scratch wound areas are masked in blue and yellow, respectively. Migration data were analyzed using two-way ANOVA and repeated measures with Bonferroni post-tests. $^{*}p < 0.05$ and $^{**}p < 0.01$ vs. FBS or PDGF; $^{\#}p < 0.05$ and $^{\#\#}p < 0.01$ vs. vehicle.

RESULTS

In vitro comparison of paclitaxel and Apt 14 in swine ECs

We first tested the effective dose range of paclitaxel for swine smooth muscle cell (SMC) migration in response to fetal bovine serum (FBS) and platelet-derived growth factor-BB (PDGF). As shown in Figure 1, paclitaxel significantly reduced the migration of FBS-stimulated (Figures 1A and 1B) and PDGF-stimulated (Figures 1C and 1D) SMCs at doses $\geq$100 nM. In addition, consistent with our previous report,[17] RNA aptamer Apt 14 significantly inhibited PDGF-mediated SMC migration, similar to the effectiveness of 100 nM paclitaxel (Figures 1C and 1E) (wound confluence at 22 h: Apt 14-PDGF, 12.68% ± 1.18%; PDGF-paclitaxel, 15.30% ± 0.79%).

To assess the effect of paclitaxel and Apt 14 RNA aptamer on EC function, we first evaluated their effect using an *in vitro* aortic EC migration assay using the same doses tested in aortic SMCs (Figure 1). It is worth noting that ECs had a higher migration rate under unstimulated (vehicle) conditions than SMCs (35% vs. 7% at 22 h). FBS induced further EC migration (Figures 2A and 2B), whereas PDGF did not (Figures 2C and 2D). Paclitaxel (1–1,000 nM) prevented FBS-mediated EC migration (Figures 2A and 2B). Paclitaxel also blunted unstimulated (vehicle) EC migration in a dose-dependent manner, with significant inhibition observed at a dose of 1 nM (Figures 2E and 2F). These data suggest that paclitaxel is more effective in preventing EC migration than SMC migration (inhibition starting dose of 1 vs. 100 nM). In contrast, despite its ability to inhibit SMC migration, Apt 14 (200 nM) had no effect on EC migration (Figure 3).

The effects of paclitaxel and Apt 14 on EC proliferation were also examined. As shown in Figure 4, FBS (2%) promoted cell proliferation (Figures 4A and 4D), whereas PDGF had no effect on the cell number after 3 days of incubation (Figure 4B). Paclitaxel inhibited serum-mediated proliferation in a dose-dependent manner (Figure 4A). In addition, incubation with higher concentrations of paclitaxel (100 nM or above) decreased cell counts compared with those in the vehicle group, indicating its cytotoxicity to ECs. However, Apt 14 did not affect EC proliferation (Figure 4C).

In vivo comparison of paclitaxel versus Apt 14 on reendothelialization

To evaluate the effect on vascular healing (reendothelialization), we delivered paclitaxel-coated balloons and Apt 14 to balloon-injured swine iliofemoral arteries using a local liquid delivery (perfusion) catheter (Figure 5). We previously showed that the perfusion catheter can effectively deliver Apt 14 to the vessel wall[18] and that Apt 14 attenuates neointimal formation in swine femoral arteries.[17] The DCB- and Apt 14-treated arteries were harvested at 14 and 28 days after treatment, with no evidence of thrombosis or dissection at the target site. En face scanning electron microscopy at 14 days demonstrated a confluent endothelium with an elongated EC morphology in the control saline- and Apt 14-treated arteries. In contrast, vessels treated with DCBs displayed cobblestone morphology, indicative of an immature endothelium. Additionally, there was significantly

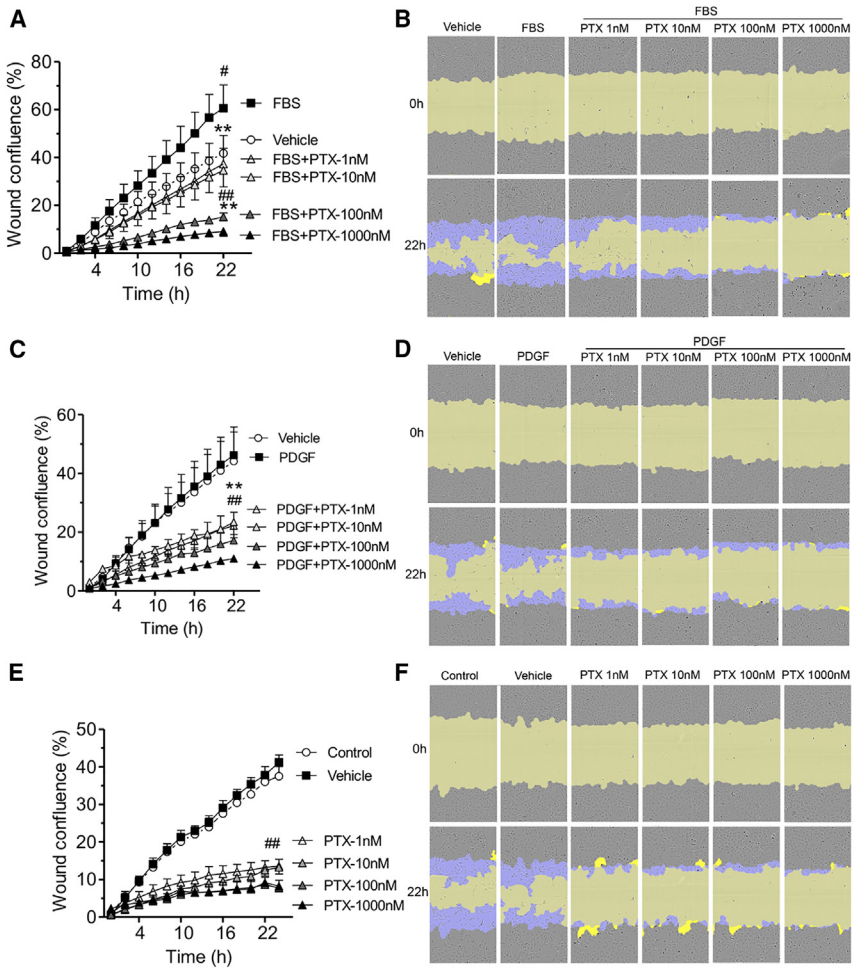

Figure 2. Effect of paclitaxel (PTX) on porcine aortic endothelial cell migration

Cells were deprived of serum for two days and then subjected to scratch wound injury and treatment. Migration was assessed on the basis of wound confluence using the IncuCyte S3 system. Cells were treated with fetal bovine serum (FBS; 2%) (A) or platelet-derived growth factor-BB (PDGF; 5 ng/mL) (C) following PTX (1–1,000 nM) or PTX alone (E). (B, D, and F) Representative cell-phase images showing wound confluence at 0 and 22 h after treatment. The initial scratch wound and scratch wound areas are masked in blue and yellow, respectively. Data were analyzed using two-way ANOVA and repeated measures with Bonferroni post-tests. *$p < 0.05$ and **$p < 0.01$ vs. FBS or PDGF; $^{\#}p < 0.05$ and $^{\#\#}p < 0.01$ vs. vehicle.

greater EC coverage in the control saline- and Apt 14-treated arteries than in the DCB-treated vessels (EC coverage at 14 days: Apt 14, 99.57% ± 0.14%; saline, 99.88% ± 0.03%; DCB, 94.20% ± 0.86%; $p < 0.001$). At 28 days, the endothelium of the control saline- and Apt 14-treated arteries maintained their confluency, while the luminal surface in the DCB-treated arteries showed significant platelet and fibrin attachment at cell junctions, consistent with an immature, dysfunctional endothelium (Figure 6) (EC coverage at 28 days: Apt 14, 99.58% ± 0.07%; saline, 98.88% ± 0.34%; DCB, 72.89% ± 1.57%; $p < 0.001$).

DISCUSSION

We report the first evidence of cell-targeted delivery of a synthetic RNA ligand to accelerate endothelial healing in a large clinically relevant vascular disease model. This study confirmed that Apt 14 had no impact on FBS- or PDGF-stimulated swine ECs, whereas paclitaxel inhibited migration and proliferation. Furthermore, the local delivery of Apt 14 *in vivo* using an endovascular approach had no impact on endothelial regrowth in a clinically relevant preclinical model.

The native vascular endothelium performs many functions to maintain a healthy patent circulatory system. ECs produce many molecules with antithrombotic properties tissue factor pathway inhibitors, nitric oxide, prostacyclin, thrombomodulin, tissue and heparin-like molecules.[19] The endothelium also produces procoagulant factors and vasoconstrictive substances, including reactive oxygen species, plasminogen activator inhibitor-1, endothelin, prostaglandin H2, TXA2, angiotensin II, and endothelium-derived cyclo-oxygenase-dependent vasoconstricting factor. In addition, a healthy confluent endothelial layer inhibits the proliferation and migration of the underlying SMCs, playing a vital role in the quiescence of the medial layer. Therefore, disruptions in healthy endothelial function prompt the initiation and progression of atherosclerosis, leading to vascular obstruction.[19]

The current preferred method for treating patients with occlusive cardiovascular disease is the endovascular approach, either using a balloon or a stent. DCBs and DESs deliver either paclitaxel or limus drugs to the luminal surface of the target artery. Currently, paclitaxel is the drug of choice for the treatment of patients with PAD. Paclitaxel, a mitotic inhibitor that stabilizes microtubules and prevents cell division, is not specific to VSMCs and thus targets all proliferating cells, including ECs.[20,21] Previous studies on coronary stents have suggested that both paclitaxel and sirolimus-eluting stents demonstrate delayed arterial healing, with a lack of complete endothelial recovery, leading to thrombotic events.[15,22] In addition, arteries treated with eluted drugs are more prone to poorly formed cell junctions with small platelet aggregations on their endothelial surface compared with non-coated BMS.[23]

In this study, we investigated Apt 14, a synthetic RNA ligand with selective VSMC binding and internalization.[16] We previously showed that Apt 14 RNA ligand functions as a smart drug by inhibiting the

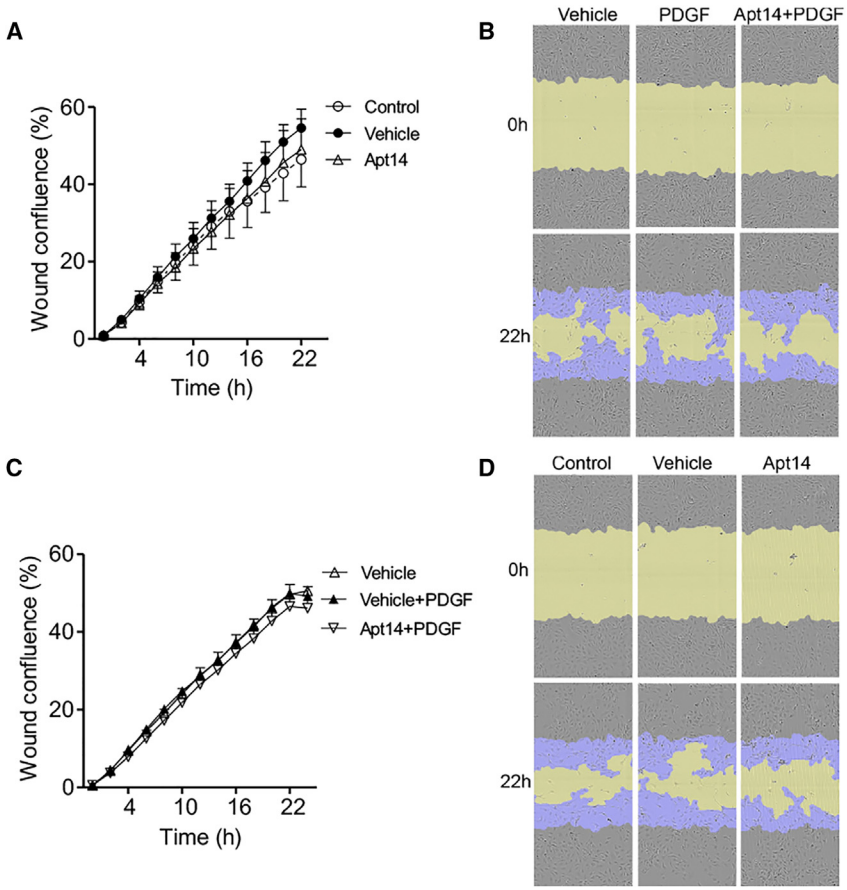

Figure 3. Effect of Apt 14 on porcine aortic endothelial cell migration

Cells were serum starved for 2 days, subjected to scratch wound injury, and treated with Apt 14 (200 nM) alone (A) or with Apt 14 followed by platelet-derived growth factor-BB (PDGF; 5 ng/mL) (C). The wound confluence was calculated using the IncuCyte S3 system. (B and D) Representative cell-phase images showing wound confluence at 0 and 22 h after treatment. The initial scratch wound and scratch wound areas are masked in blue and yellow, respectively. Migration data were analyzed using two-way ANOVA and repeated measures, with Bonferroni post hoc tests.

activation of phosphatidylinositol 3-kinase/protein kinase-B (P13K/Akt).[16] Here we showed that Apt 14 had no impact on the proliferation or migration of PDGF-stimulated swine ECs, whereas paclitaxel inhibited both the proliferation and migration of ECs. To further evaluate the effect of Apt 14 on the endothelium, we used a clinically relevant large animal model. Previously, we showed successful delivery of the aptamer using a liquid delivery catheter in an *ex vivo* swine artery model.[18] In addition, we demonstrated that Apt 14 inhibited vascular remodeling and neointimal growth in a swine iliofemoral injury model.[17]

For our experiments, a preclinical reendothelialization animal model was used, as it has been shown to provide insights into the impact of endovascular drug delivery devices on reendothelialization and vascular healing.[23] Most of these studies focused on traditional antiproliferative drugs, such as paclitaxel and limus-based drugs coated onto stent platforms, and have demonstrated that both drugs inhibit or delay reendothelialization, compared with non-drug-coated controls.[24,25] Herein, we compared endothelial recovery after intraluminal delivery of Apt 14 to a paclitaxel-coated balloon, a currently used treatment option for PAD. No additional controls were used, given that our previous studies demonstrated that only Apt 14 is retained within the wall and inhibits neointimal growth compared with nonspecific aptamers.[17,18] Electron microscopic analysis revealed that at 14 days, Apt 14-treated arteries demonstrated a confluent, elongated endothelium, whereas DCB-treated arteries showed areas of incomplete reendothelialization with a cobblestone morphology, indicating an immature endothelium. At 28 days, Apt 14-treated arteries continued to show complete reendothelialization, while the luminal surface in DCB-treated arteries showed platelet/fibrin attachment at the junctions, indicating immature and dysfunctional endothelium. These data confirm faster and more complete EC healing in Apt 14-treated arteries than in DCB-treated vessels, which is the current standard of care.

As previously mentioned, the goals of this study were to confirm that Apt 14 had no impact on endothelial regrowth and to compare vascular healing with the current gold standard, paclitaxel-coated balloons. Our results showed that Apt 14 delivery did not affect endothelial regrowth, whereas arteries treated with paclitaxel-coated balloons showed platelet and fibrin deposition at the endothelial junctions, which has not been demonstrated previously. We attribute these results to the selectivity of the aptamer to SMCs, which maintain EC function and reendothelialization (i.e., healing) of the artery. Antiproliferative drugs such as paclitaxel are cytotoxic, altering the natural healing process and triggering secondary inflammatory reactions.[26] Additionally, the endovascular approach of Apt 14 delivers liquid therapy directly to the medial wall, which differs from the DCB technique, in which paclitaxel is deposited on the luminal surface. In particular, as these platforms use the crystalline form of paclitaxel, the antiproliferative drug may not be bioavailable (i.e., solubilized) for uptake by VSMCs for days, weeks, or months and thus can disrupt the natural reendothelialization process.

Although our results demonstrated the successful delivery of Apt 14 and endothelial regrowth, the study was limited to using healthy (non-diseased) arteries. The therapy will need to be evaluated in arteries more similar to diseased human lesions, which are more complex and often include fibrosis and a necrotic core with calcification or hemorrhage. Additionally, severe diseased lesions require de-bulking

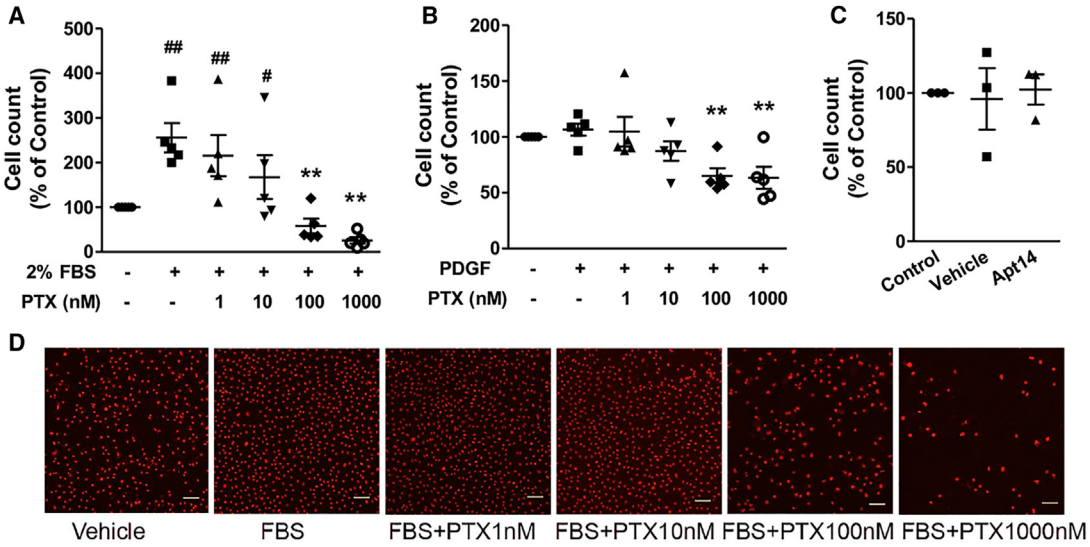

Figure 4. Effects of paclitaxel (PTX) and Apt 14 on porcine aortic endothelial cell proliferation

Cells were treated for 3 days with fetal bovine serum (FBS; 2%) (A) or platelet-derived growth factor-BB (PDGF; 10 ng/mL) (B) following PTX (1–1,000 nM) or Apt 14 (200 nM) (C). Propidium iodide (PI) nucleic acid stain-labeled nuclei were used for cell counting. (D) Representative images of PI-positive nuclei 3 days after treatment. Data were analyzed using one-way ANOVA with Tukey's post hoc test. $^{**}p < 0.01$ vs. FBS or PDGF; $^{\#}p < 0.05$ and $^{\#\#}p < 0.01$ vs. vehicle. Scale bar: 100 μm.

via atherectomy or cutting-balloon devices, which may alter aptamer delivery and retention.

In conclusion, these results provide the first evidence of an RNA ligand that accelerates endothelial healing in a large clinically relevant animal model. The cell-specific targeted approach may be more effective and overcome some of the safety concerns compared with conventional non-targeted drugs. Our local liquid delivery approach is complementary to the RNA aptamer delivering the cell-specific therapy directly to the medial wall, achieving the preferred "leave nothing behind" strategy in treating patients with occlusive arterial disease.

MATERIALS AND METHODS

Reagents

High-glucose Dulbecco's modified Eagle's medium (DMEM) (catalog #11965), phenol red-free DMEM (catalog #31053), L-glutamine (catalog #25030-081), Minimum Essential Medium Non-Essential Amino Acids (MEM-NEAA; catalog #11140), penicillin/streptomycin (catalog #15140-122), and Dulbecco's PBS (DPBS; catalog #14190-144) were purchased from Gibco (Grand Island, NY). Complete EC medium/w kit (catalog #M1168) was purchased from Cell Biologics (Chicago, IL). FBS (catalog #F2442), mouse PDGF (catalog #SRP3229), and paclitaxel (catalog #T7191) were purchased from Sigma (St. Louis, MO). Propidium iodide (PI; catalog #P3566) was purchased from Molecular Probes (Eugene, OR). Apt 14 was chemically synthesized by Integrated DNA Technologies (Coralville, IA).

Cell culture

Primary porcine aortic SMCs were isolated from the aorta by enzymatic digestion as described previously[17] and cultured in DMEM containing 10% FBS, 1× MEM-NEAA, and 1× penicillin/streptomycin in a humidified atmosphere containing 5% CO_2 at 37°C. Primary porcine aortic ECs were purchased from Cell Biologics (catalog #P-6052) and cultured in complete EC medium containing 2% FBS and growth factors. In the protocols described below, cells were synchronized for two days in serum-free DMEM (SMCs) or endothelial medium without FBS and growth factors (ECs) before treatment. Paclitaxel (1–1,000 nM) or vehicle (0.05% ethanol) was applied to the cells following FBS (5% for SMCs and 2% for ECs) or PDGF treatment. Apt 14 (200 nM) or vehicle (4% 1×BB) was administered 30 min before FBS or PDGF.

RNA aptamers

RNA Apt 14 was chemically synthesized by Integrated DNA Technologies using 5′ C12-NH2 and 2′ fluoropyrimidines. The sequence of Apt 14 is as follows: 5′-GGGAGGACGAUGCGGGCCUUUCGUU CUGACCUCCCCAGACGACUCGCCCGA -3′.

Before being applied to cells, Apt 14 was folded at 5 μM in 1× binding buffer (1×BB, 20 mM HEPES, 150 mM NaCl, and 2 mM $CaCl_2$) at 37°C for 20–30 min and diluted in serum-free medium.

Migration assays

Cell migration was evaluated by the scratch wound assay using the WoundMaker-IncuCyte ZOOM-ImageLock plate system (Sartorius AG, Göttingen, Germany). Cells were seeded in 96-well plates at 15,000 cells per well in complete growth medium for one day and then synchronized in serum-free medium for two days. After the scratch wound was made using the WoundMaker, the indicated treatments were administered to the cells in a serum-free medium. The

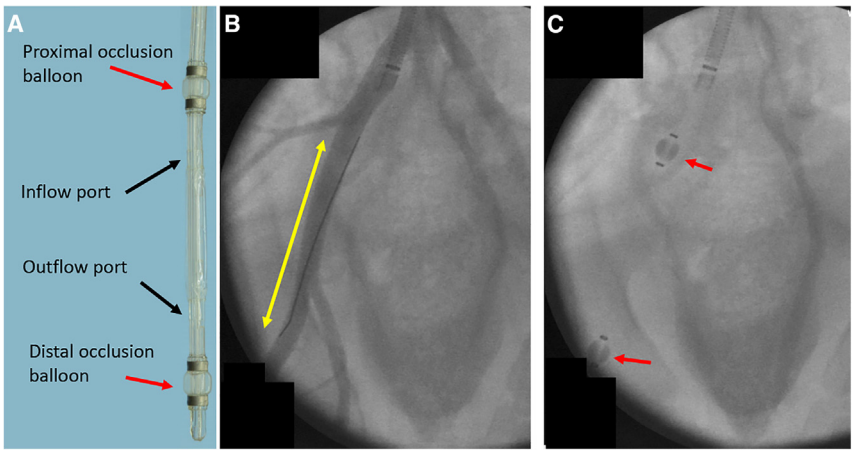

Figure 5. Local delivery using a perfusion catheter
(A) The perfusion catheter isolates the treatment area by deployment of the proximal and distal occlusion balloons and infusion of the treatment is accomplished through the inflow port. (B) Angiographic image of the treatment area. The yellow double-arrow shows the treatment area, within the external iliac artery. (C) Angiographic image showing the position of the perfusion catheter in its deployed state. The red arrows indicate the location of the proximal and distal occlusion balloons.

plates were then placed in IncuCyte S3, and phase images of the cells were taken every 2 h. The images were processed, and wound confluence (percentage) within the wound region was calculated using IncuCyte Analysis Software (2021 B). Each treatment was conducted in duplicate or triplicate.

Proliferation assays

Cell proliferation was determined by counting the number of cells obtained from nuclei using PI nucleic acid staining. Porcine ECs were seeded in 96-well plates at 4,000 cells per well in complete medium for 1 day and then starved in serum-free medium for 2 days before treatment. After treatment for 3 days, the cells were fixed with ice-cold methanol for 5 min at room temperature and then incubated with 750 nM PI in DPBS for 30 min. The plates were placed in IncuCyte, and red fluorescent images were captured using a 4× magnifying lens. The images were processed, and the number of nuclei in each image was counted using IncuCyte Analysis Software (2021 B). Each treatment was conducted in duplicate or triplicate.

Pig injury model

This study was approved by the Institutional Animal Care and Use Committee (IACUC), conformed to the current Guide for the Care and Use of Laboratory Animals, and complied with the ARRIVE (Animal Research: Reporting of *In Vivo* Experiments) guidelines. The experimental preparation of the animal model has been previously reported.[27–29] Six female pigs (12.3–14.1 kg) were pre-medicated with ketamine and midazolam, intubated, and placed on a ventilator. While the animals were ventilated under isoflurane gas anesthesia, the right carotid artery was exposed under a sterile field. The caudal end of the right carotid artery was tied off. A small incision was made in the right carotid artery with micro-scissors, and a 6 Fr guide sheath was inserted. A NITREX 0.014 inch guidewire (ev3 Inc., Plymouth, MN) was inserted, and under fluoroscopic guidance, endothelial denudation using a 4 × 12 mm angioplasty balloon catheter (Abbott Vascular, Abbott Park, IL) was performed on the left and right iliac arteries. Following denudation, the arteries were treated with either a paclitaxel-coated balloon (IN.PACT Admiral, Medtronic, Minneapolis, MN) or a liquid delivery catheter (5.0 × 40 mm; Advanced Catheter Therapies, Chattanooga, TN) delivering Apt 14 or saline. DCB was delivered at a pressure based on the manufacturer's recommendation for two minutes. Apt 14 and saline were delivered at a luminal delivery pressure of 0.15 atm for two minutes. The perfusion catheter locally delivered 2.5 mL aptamer at a concentration of 500 nM. The perfusion catheter had two compliant occlusion balloons (proximal and distal) that defined the treatment chamber. Luminal pressure, or treatment chamber pressure, was measured in real time using a sensor located within the treatment chamber, which was connected to an external pressure monitor to monitor the pressure during the infusion of the liquid drug. Two animals and four arteries were treated with Apt 14, saline, or DCB for each group. Antiplatelet therapy consisted of aspirin (40 mg) and clopidogrel (150 mg) administered orally 24 h before catheterization, while single-dose intra-arterial heparin (150 IU/kg) and lidocaine were administered at the time of catheterization. During the duration of the study, aspirin (40 mg/day) and clopidogrel (81 mg/day) were continuously provided. Fourteen and twenty-eight days after treatment, the anesthetized animals were euthanized and the treated segments were removed on the basis of landmarks identified by angiography. The arteries were perfused with saline and formalin fixed under physiological pressure before removal. The segments were stored in 10% formalin at room temperature and then processed for scanning electron microscopy.

Scanning electron microscopic analysis

To visualize the arterial surface following deployment, the formalin-fixed arteries were first dehydrated in a graded series of ethanol. After critical point drying, tissue samples were mounted and sputter-coated with gold. The specimens were visualized using a Phenom XL scanning electron microscope (Thermo Fisher Scientific, Waltham, MA). Endothelial surface coverage was quantified using color threshold analysis (ImageJ; National Institutes of Health).

Statistical analysis

All values are expressed as mean ± SE. Continuous variables were compared between groups using one- or two-way ANOVA using Prism 9 (GraphPad Software, La Jolla, CA). Differences were considered to be statistically significant at $p \leq 0.05$. If statistical significance was shown, a comparison of quantitative data of multiple groups was

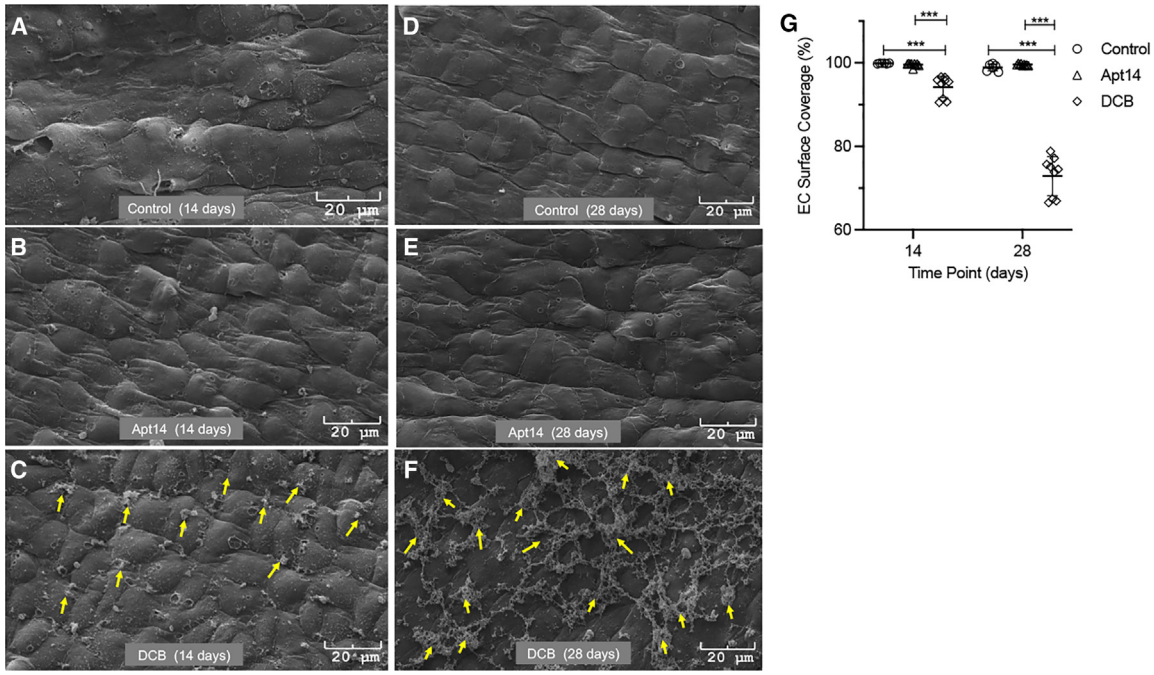

Figure 6. Vascular healing following RNA aptamer delivery versus drug-coated balloon (DCB)

(A–F) Representative 14 and 28 day scanning electron microscopic (SEM) images of arteries treated with Apt 14, DCB, and control (no drugs, balloon injury only). At 14 days post-treatment, Apt 14-treated arteries display elongated, complete endothelialization similar to that in control segments, but DCB-treated arteries show cobble-stone endothelia with platelet attachments at their boundaries (yellow arrows). At 28 days post-treatment, Apt 14-treated arteries maintain their elongated morphometry with no platelet adherence. The DCB-treated arteries show platelet/fibrin adherence at EC junctions (yellow arrows). Blood flowed from right to left. (G) Surface coverage graph based on morphometric (color threshold, ImageJ) analysis of the Apt 14-, DCB-, and saline (control)-treated arteries. ***$p < 0.001$ vs. control or DCB.

performed using Tukey's multiple-comparisons post hoc test or the Bonferroni post hoc test.

DATA AND CODE AVAILABILITY

The data supporting the findings of this study are available from the corresponding authors upon reasonable request.

ACKNOWLEDGMENTS

F.J.M. was supported by the Office of Research and Development, the Department of Veterans Affairs (grant I01BX001729), and the National Institutes of Health (grant 1R01EB028798). S.K.Y. is supported by the National Institutes of Health (grant 1R01EB028798). The content of this manuscript is solely the responsibility of the authors, and does not necessarily represent the official views of the granting agencies.

AUTHOR CONTRIBUTIONS

Writing – Original Conceptualization, S.K.Y., P.H.G., and F.J.M.; Methodology, S.K.Y., B.L., L.S., and F.J.M.; Data Acquisition, Curation, and Analysis, S.K.Y., L.L., L.S., B.L., and F.J.M.; Resources, S.K.Y. and F.J.M.; Writing – Original Draft, S.K.Y., B.L., and F.J.M.; Writing – Review & Editing, S.K.Y., L.L., L.S., P.H.G., and F.J.M.; Supervision, S.K.Y. and F.J.M.

DECLARATION OF INTERESTS

S.K.Y. serves on the Scientific Advisory Board of Advanced Catheter Therapies and has received grant support from Advanced Catheter Therapies, Alucent Biomedical, Toray Industries, Biosensors International, Advanced NanoTherapies, OrbusNeich Medical, and Becton Dickinson.

REFERENCES

1. Mahoney, E.M., Wang, K., Keo, H.H., Duval, S., Smolderen, K.G., Cohen, D.J., Steg, G., Bhatt, D.L., and Hirsch, A.T.; Reduction of Atherothrombosis for Continued Health REACH Registry Investigators (2010). Vascular hospitalization rates and costs in patients with peripheral artery disease in the United States. Circulation. Circ. Cardiovasc. Qual. Outcomes *3*, 642–651. https://doi.org/10.1161/circoutcomes.109.930735.

2. Adam, D.J., Beard, J.D., Cleveland, T., Bell, J., Bradbury, A.W., Forbes, J.F., Fowkes, F.G.R., Gillepsie, I., Ruckley, C.V., Raab, G., and Storkey, H.; BASIL trial participants (2005). Bypass versus angioplasty in severe ischaemia of the leg (BASIL): multicentre, randomised controlled trial. Lancet *366*, 1925–1934. https://doi.org/10.1016/s0140-6736(05)67704-5.

3. Conte, M.S., Bandyk, D.F., Clowes, A.W., Moneta, G.L., Seely, L., Lorenz, T.J., Namini, H., Hamdan, A.D., Roddy, S.P., Belkin, M., et al.; PREVENT III Investigators (2006). Results of PREVENT III: a multicenter, randomized trial of edifoligide for the prevention of vein graft failure in lower extremity bypass surgery. J. Vasc. Surg. *43*, 742–751. https://doi.org/10.1016/j.jvs.2005.12.058.

4. Schillinger, M., Sabeti, S., Loewe, C., Dick, P., Amighi, J., Mlekusch, W., Schlager, O., Cejna, M., Lammer, J., and Minar, E. (2006). Balloon angioplasty versus implantation of nitinol stents in the superficial femoral artery. N. Engl. J. Med. *354*, 1879–1888. https://doi.org/10.1056/NEJMoa051303.

5. Schillinger, M., Sabeti, S., Dick, P., Amighi, J., Mlekusch, W., Schlager, O., Loewe, C., Cejna, M., Lammer, J., and Minar, E. (2007). Sustained benefit at 2 years of primary femoropopliteal stenting compared with balloon angioplasty with optional stenting. Circulation *115*, 2745–2749. https://doi.org/10.1161/circulationaha.107.688341.

6. Norgren, L., Hiatt, W.R., Dormandy, J.A., Nehler, M.R., Harris, K.A., Fowkes, F.G.R., TASC II Working Group, Bell, K., Caporusso, J., Durand-Zaleski, I., Komori, K., Lammer, J., Liapis, C., Novo, S., Razavi, M., Robbs, J., Schaper, N., Shigematsu, H., Sapoval, M., White, C., White, J., Clement, D., Creager, M., Jaff, M., Mohler, E., 3rd, Rutherford, R.B., Sheehan, P., Sillesen, H., and Rosenfield, K. (2007). Inter-Society Consensus for the Management of Peripheral Arterial Disease (TASC II). Eur. J. Vasc. Endovasc. Surg. *33* (*Suppl 1*), S1–S75. https://doi.org/10.1016/j.ejvs.2006.09.024.

7. Tsetis, D., and Belli, A.M. (2004). Guidelines for stenting in infrainguinal arterial disease. Cardiovasc. Intervent. Radiol. *27*, 198–203. https://doi.org/10.1007/s00270-004-0029-1.

8. Tosaka, A., Soga, Y., Iida, O., Ishihara, T., Hirano, K., Suzuki, K., Yokoi, H., Nanto, S., and Nobuyoshi, M. (2012). Classification and clinical impact of restenosis after femoropopliteal stenting. J. Am. Coll. Cardiol. *59*, 16–23. https://doi.org/10.1016/j.jacc.2011.09.036.

9. Stone, G.W., Ellis, S.G., Cox, D.A., Hermiller, J., O'Shaughnessy, C., Mann, J.T., Turco, M., Caputo, R., Bergin, P., Greenberg, J., et al.; TAXUS-IV Investigators (2004). A polymer-based, paclitaxel-eluting stent in patients with coronary artery disease. N. Engl. J. Med. *350*, 221–231. https://doi.org/10.1056/NEJMoa032441.

10. Morice, M.C., Serruys, P.W., Sousa, J.E., Fajadet, J., Ban Hayashi, E., Perin, M., Colombo, A., Schuler, G., Barragan, P., Guagliumi, G., et al.; RAVEL Study Group. Randomized Study with the Sirolimus-Coated Bx Velocity Balloon-Expandable Stent in the Treatment of Patients with de Novo Native Coronary Artery Lesions (2002). A randomized comparison of a sirolimus-eluting stent with a standard stent for coronary revascularization. N. Engl. J. Med. *346*, 1773–1780. https://doi.org/10.1056/NEJMoa012843.

11. Scheinert, D., Scheinert, S., Sax, J., Piorkowski, C., Bräunlich, S., Ulrich, M., Biamino, G., and Schmidt, A. (2005). Prevalence and clinical impact of stent fractures after femoropopliteal stenting. J. Am. Coll. Cardiol. *45*, 312–315. https://doi.org/10.1016/j.jacc.2004.11.026.

12. Hwang, C.W., Wu, D., and Edelman, E.R. (2001). Physiological transport forces govern drug distribution for stent-based delivery. Circulation *104*, 600–605.

13. Katsanos, K., Spiliopoulos, S., Kitrou, P., Krokidis, M., and Karnabatidis, D. (2018). Risk of Death Following Application of Paclitaxel-Coated Balloons and Stents in the Femoropopliteal Artery of the Leg: A Systematic Review and Meta-Analysis of Randomized Controlled Trials. J. Am. Heart Assoc. *7*, e011245. https://doi.org/10.1161/JAHA.118.011245.

14. Vorpahl, M., Yazdani, S.K., Nakano, M., Ladich, E., Kolodgie, F.D., Finn, A.V., and Virmani, R. (2010). Pathobiology of stent thrombosis after drug-eluting stent implantation. Curr. Pharmaceut. Des. *16*, 4064–4071.

15. Finn, A.V., Joner, M., Nakazawa, G., Kolodgie, F., Newell, J., John, M.C., Gold, H.K., and Virmani, R. (2007). Pathological correlates of late drug-eluting stent thrombosis: strut coverage as a marker of endothelialization. Circulation *115*, 2435–2441. https://doi.org/10.1161/circulationaha.107.693739.

16. Thiel, W.H., Esposito, C.L., Dickey, D.D., Dassie, J.P., Long, M.E., Adam, J., Streeter, J., Schickling, B., Takapoo, M., Flenker, K.S., et al. (2016). Smooth Muscle Cell-targeted RNA Aptamer Inhibits Neointimal Formation. Mol. Ther. *24*, 779–787. https://doi.org/10.1038/mt.2015.235.

17. Yazdani, S.K., Lei, B., Cawthon, C.V., Cooper, K., Huett, C., Giangrande, P.H., and Miller, F.J., Jr. (2022). Local intraluminal delivery of a smooth muscle-targeted RNA ligand inhibits neointima growth in a porcine model of peripheral vascular disease. Mol. Ther. Nucleic Acids *29*, 577–583. https://doi.org/10.1016/j.omtn.2022.08.007.

18. Udofot, O., Lin, L.H., Thiel, W.H., Erwin, M., Turner, E., Miller, F.J., Jr., Giangrande, P.H., and Yazdani, S.K. (2019). Delivery of Cell-Specific Aptamers to the Arterial Wall with an Occlusion Perfusion Catheter. Molecular therapy. Nucleic acids *16*, 360–366. https://doi.org/10.1016/j.omtn.2019.03.005.

19. Otsuka, F., Finn, A.V., Yazdani, S.K., Nakano, M., Kolodgie, F.D., and Virmani, R. (2012). The importance of the endothelium in atherothrombosis and coronary stenting. Nat. Rev. Cardiol. *9*, 439–453. https://doi.org/10.1038/nrcardio.2012.64.

20. Axel, D.I., Kunert, W., Göggelmann, C., Oberhoff, M., Herdeg, C., Küttner, A., Wild, D.H., Brehm, B.R., Riessen, R., Köveker, G., and Karsch, K.R. (1997). Paclitaxel inhibits arterial smooth muscle cell proliferation and migration *in vitro* and *in vivo* using local drug delivery. Circulation *96*, 636–645.

21. Rowinsky, E.K., and Donehower, R.C. (1995). Paclitaxel (taxol). N. Engl. J. Med. *332*, 1004–1014. https://doi.org/10.1056/nejm199504133321507.

22. Joner, M., Finn, A.V., Farb, A., Mont, E.K., Kolodgie, F.D., Ladich, E., Kutys, R., Skorija, K., Gold, H.K., and Virmani, R. (2006). Pathology of drug-eluting stents in humans: delayed healing and late thrombotic risk. J. Am. Coll. Cardiol. *48*, 193–202.

23. Joner, M., Nakazawa, G., Finn, A.V., Quee, S.C., Coleman, L., Acampado, E., Wilson, P.S., Skorija, K., Cheng, Q., Xu, X., et al. (2008). Endothelial cell recovery between comparator polymer-based drug-eluting stents. J. Am. Coll. Cardiol. *52*, 333–342.

24. Nakazawa, G., Finn, A.V., John, M.C., Kolodgie, F.D., and Virmani, R. (2007). The significance of preclinical evaluation of sirolimus-paclitaxel-and zotarolimus-eluting stents. Am. J. Cardiol. *100*, 36m–44m. https://doi.org/10.1016/j.amjcard.2007.08.020.

25. Silva, G.V., Fernandes, M.R., Madonna, R., Clubb, F., Oliveira, E., Jimenez-Quevedo, P., Branco, R., Lopez, J., Angeli, F.S., Sanz-Ruiz, R., et al. (2009). Comparative healing response after sirolimus- and paclitaxel-eluting stent implantation in a pig model of restenosis. Cathet. Cardiovasc. Interv. *73*, 801–808. https://doi.org/10.1002/ccd.21879.

26. Stampfl, U., Radeleff, B., Sommer, C., Stampfl, S., Lopez-Benitez, R., Thierjung, H., Kurz, P., Berger, I., and Richter, G.M. (2009). Paclitaxel-induced arterial wall toxicity and inflammation: part 2--long-term tissue response in a minipig model. J. Vasc. Intervent. Radiol. *20*, 1608–1616. https://doi.org/10.1016/j.jvir.2009.08.019.

27. Yazdani, S.K., Sheehy, A., Nakano, M., Nakazawa, G., Vorpahl, M., Otsuka, F., Donn, R.S., Perkins, L.E., Simonton, C.A., Kolodgie, F.D., and Virmani, R. (2013). Preclinical evaluation of second-generation everolimus- and zotarolimus-eluting coronary stents. J. Invasive Cardiol. *25*, 383–390.

28. Turner, E., Erwin, M., Atigh, M., Christians, U., Saul, J.M., and Yazdani, S.K. (2018). *In vitro* and *in vivo* Assessment of Keratose as a Novel Excipient of Paclitaxel Coated Balloons. Front. Pharmacol. *9*, 808. https://doi.org/10.3389/fphar.2018.00808.

29. Atigh, M.K., Goel, E., Erwin, M., Greer, R., 2nd, Ohayon, J., Pettigrew, R.I., and Yazdani, S.K. (2021). Precision delivery of liquid therapy into the arterial wall for the treatment of peripheral arterial disease. Sci. Rep. *11*, 18676. https://doi.org/10.1038/s41598-021-98063-z.